

PERISTALTIC FLOW OF MHD PHAN-THIEN-TANNER FLUID IN AN ASYMMETRIC CHANNEL WITH POROUS MEDIUM

S.V.H.N. KRISHNA KUMARI P.

Professor, Department of Mathematics, Vidya Jyothi Institute of Technology, Hyderabad, India

SAROJ VERNEKAR

Asst. Professor, Stanley College of Engineering and Technology for Women, Hyderabad, India

AND

Y.V.K. RAVI KUMAR

Practice School Division, Birla Institute of Technology & Science -Pilani, Hyderabad, India

RECEIVED : 21 March, 2016

This paper deals with effect of magnetic field and porous medium on peristaltic transport of Phan-Thien-Tanner fluid in an asymmetric channel induced by sinusoidal peristaltic waves traveling down the flexible walls of the channel. The flow is investigated in a wave frame of reference moving with the velocity of the wave by using the long wavelength and low Reynolds number approximations. The nonlinear governing equations are solved employing a perturbation method by choosing We as the perturbation parameter. The expressions for velocity and pressure gradient are obtained. The features of the flow characteristics are analyzed through graphs and the obtained results are discussed in detail.

KEYWORDS : Peristaltic transport; Phan-Thien-Tanner fluid; Porous medium; Asymmetric channel.

INTRODUCTION

It is well known that mixing and transporting of physiological fluids is referred as peristalsis, which is generated due to progressive waves of area contraction and expansion along the length of a distensible tube containing fluid. Peristalsis occurs widely in the functioning of the ureter, food mixing and chyme movement in the intestine, movement of eggs in the fallopian tube, the transport of the spermatozoa in cervical canal, transport of bile in the bile duct, transport of cilia, and circulation of blood in small blood vessels. The peristaltic transport through tubes /channels have attracted considerable attention due to their wide applications in medical and engineering sciences, such as, in physiology, roller and finger pumps, sanitary fluid transport, transport of corrosive fluids etc.

Flow through a porous medium has several practical applications especially in geophysical fluid dynamics. Examples of natural porous media are beach sand, sandstone, limestone, the human lung, bile duct, gall bladder with stones in small blood vessels. The magneto hydrodynamic peristaltic flow in a channel has a pivotal role in the motion of physiological fluids including blood and blood pump machines. Motivated by these facts, a good number of analytical, numerical and experimental [1-10] studies have been conducted to

understand peristaltic action under different conditions with reference to physiological and mechanical situations.

Elad [11] have developed a mathematical model for wall-induced peristaltic fluid flow in a channel with wave trains having phase difference on the upper and lower walls. The studies on the different non-Newtonian fluid models were carried out by several investigators [12-15]. Misra *et al.* [16] studied the peristaltic transport of a physiological fluid in an asymmetric porous channel in the presence of an external magnetic field. However, Shit and Roy [17] investigated the effect of induced magnetic field on peristaltic flow of a micropolar fluid in an asymmetric channel. Peristaltic flow of non-Newtonian fluids in a tube was first studied by Raju and Devanathan [18]. Ravi Kumar *et. al* [19] studied the unsteady peristaltic pumping in a finite length tube with permeable wall. Ravi Kumar *et. al* [20] studied the peristaltic pumping of a magneto hydrodynamic Casson fluid in an inclined channel. Ravi Kumar *et. al* [21] studied the peristaltic pumping of a Jeffrey fluid under the effect of a magnetic field in an inclined channel. Ravi Kumar *et. al* [22] studied the effects of Slip and Heat Transfer on the Peristaltic Pumping of a Williamson Fluid in an Inclined Channel.

In view of the importance of the peristaltic transport of a non Newtonian fluid in an asymmetric channel with porous medium, we considered the problem by taking Phan-Thien-Tanner Fluid model. The effect of various parameters of interest on the flow characteristics is studied.

MATHEMATICAL FORMULATION

We consider an incompressible Phan-Thien-Tanner fluid flow in an asymmetric channel with porous medium, of width $d_1 + d_2$ and a uniform magnetic field B_0 which is applied in the transverse direction to the flow. Let c be the speed by which sinusoidal wave trains propagate along the channel walls. Consider the rectangular coordinate system (X, Y) where X and Y axes are taken respectively parallel and transverse to the direction of wave propagation. The wall surfaces are modeled by

$$\bar{Y} = H_1 = d_1 + a_1 \cos \left[\frac{2\pi}{\lambda} (X\bar{c} - \bar{t}) \right], \bar{Y} = H_2 = -d_1 - b_1 \cos \left[\frac{2\pi}{\lambda} (X\bar{c} - \bar{t}) + \phi \right] \dots (2.1)$$

where ϕ is the phase varying in the range $0 \leq \phi \leq \pi$. Here, $\phi = 0$ corresponds to symmetric channel with waves out of phase and $\phi = \pi$ with waves in phase, and further $a_1^2 + b_1^2 + 2a_1b_1 \cos \phi \leq (d_1 + d_2)^2$ so that walls will not intersect with each other. The basic equations of motion of fluid are as follows:

Continuity equation

$$\Delta V = 0 \quad \dots (2.2)$$

Momentum equation

$$\rho \frac{dv}{dt} = \text{div } T \quad \dots (2.3)$$

The constitutive equations for PTT model are

$$T = -pI + S \quad \dots (2.4)$$

$$f(\text{tr}(s))s + ks^\nabla = 2\mu D \quad \dots (2.5)$$

$$s^\nabla = \frac{ds}{dt} - s \cdot L^* - L \cdot s, \quad \dots (2.6)$$

$$L = \text{grad } V, \quad \dots (2.7)$$

where p is the pressure, \mathbf{I} is the identity tensor, \mathbf{V} is the velocity, \mathbf{T} is the Cauchy stress tensor, μ is the dynamic viscosity, \mathbf{s} is an extra-stress tensor, \mathbf{D} is the deformation rate tensor, k is the relaxation time, s^∇ denotes Oldroyd's upper-convected derivative, d/dt the material derivative, tr is the trace and asterisk denotes the transpose. Function f is the linear PTT model which satisfies

$$f(\text{tr}(s)) = 1 + \frac{\epsilon k}{\mu} \text{tr}(s) \quad \dots (2.8)$$

Note that the PTT model reduces to an Upper Convicted Maxwell model (UCM) when the extensional parameter ϵ is zero. The transformations between fixed frame to wave frame is given by

$$x = \bar{X} - ct; y = \bar{Y}; u(x, y) = U(\bar{X} - ct, Y); v(x, y) = V(\bar{X} - ct, Y), \bar{p}(x) = \bar{P}(\bar{X}, t) \quad \dots (2.9)$$

Using the equation (2.9) the governing equations in the wave frame can be written as

$$\frac{\partial \bar{u}}{\partial x} + \frac{\partial \bar{v}}{\partial y} = 0 \quad \dots (2.10)$$

$$\rho \left[\bar{u} \frac{\partial}{\partial x} + \bar{v} \frac{\partial}{\partial y} \right] \bar{u} = -\frac{\partial \bar{p}}{\partial x} + \frac{\partial \bar{S}_{xx}}{\partial y} + \frac{\partial \bar{S}_{xy}}{\partial x} - \left(\frac{\mu}{k_0} + \mu_e^2 B_0^2 \right) (\bar{u} + c) \quad \dots (2.11)$$

$$\rho \left[\bar{u} \frac{\partial}{\partial x} + \bar{v} \frac{\partial}{\partial y} \right] \bar{v} = -\frac{\partial \bar{p}}{\partial x} + \frac{\partial \bar{S}_{yx}}{\partial y} + \frac{\partial \bar{S}_{xy}}{\partial x} - \frac{\mu}{k_0} \bar{v} \quad \dots (2.12)$$

$$f \bar{S}_{xy} + k \left[\bar{u} \frac{\partial \bar{S}_{xx}}{\partial x} + \bar{v} \frac{\partial \bar{S}_{xx}}{\partial y} - 2 \frac{\partial \bar{u}}{\partial y} \bar{S}_{xx} - 2 \frac{\partial \bar{u}}{\partial x} \bar{S}_{xy} \right] \bar{v} = 2\mu \frac{\partial \bar{u}}{\partial x} \quad \dots (2.13)$$

$$f \bar{S}_{xy} + k \left[\bar{u} \frac{\partial \bar{S}_{yy}}{\partial x} + \bar{v} \frac{\partial \bar{S}_{yy}}{\partial y} - 2 \frac{\partial \bar{v}}{\partial y} \bar{S}_{yx} - 2 \frac{\partial \bar{v}}{\partial x} \bar{S}_{yy} \right] \bar{v} = 2\mu \frac{\partial \bar{v}}{\partial y} \quad \dots (2.14)$$

$$f \bar{S}_{zz} + k \left[\bar{u} \frac{\partial \bar{S}_{zz}}{\partial x} + \bar{v} \frac{\partial \bar{S}_{zz}}{\partial y} \right] = 0 \quad \dots (2.15)$$

$$f \bar{S}_{xy} + k \left[\bar{u} \frac{\partial \bar{S}_{xy}}{\partial x} + \bar{v} \frac{\partial \bar{S}_{xy}}{\partial y} - \frac{\partial \bar{v}}{\partial x} \bar{S}_{xx} - \frac{\partial \bar{v}}{\partial y} \bar{S}_{xy} - \frac{\partial \bar{u}}{\partial x} \bar{S}_{xy} - \frac{\partial \bar{u}}{\partial y} \bar{S}_{yy} \right] \bar{v} = \mu \left(\frac{\partial \bar{u}}{\partial y} + \frac{\partial \bar{v}}{\partial x} \right) \quad \dots (2.16)$$

$$f = 1 + \frac{\epsilon k}{\mu} (\bar{S}_{xx} + \bar{S}_{yy} + \bar{S}_{zz}) \quad \dots (2.17)$$

The boundary conditions are

$$\bar{\psi} = \frac{q}{2}, \bar{u} = \frac{\partial \bar{\psi}}{\partial y} = -c \text{ at } \bar{y} = H_1, \quad \bar{\psi} = -\frac{q}{2}, \bar{u} = \frac{\partial \bar{\psi}}{\partial y} = -c \text{ at } \bar{y} = H_2 \dots (2.18)$$

The non-dimensional quantities and the expressions for velocity in terms of stream function are given by

$$\begin{aligned} x = \frac{\bar{x}}{\lambda}, \quad y = \frac{\bar{y}}{d_1}, \quad u = \frac{\bar{u}}{c}, \quad v = \frac{\bar{v}}{\delta c}, \quad \delta = \frac{d_1}{\lambda}, \quad p = \frac{d_1^2 \bar{p}}{\mu c \lambda}, \quad t = \frac{c \bar{t}}{\lambda}, \quad h_1 = \frac{H_1}{d_1}, \quad h_2 = \frac{H_2}{d_1}, \\ \text{Re} = \frac{\rho c d_1}{\mu}, \quad d = \frac{d_2}{d_1}, \quad a = \frac{a_1}{d_1}, \quad b = \frac{b_1}{d_1}, \quad S_{ij} = \frac{\bar{S}_{ij} d_1}{\mu c}, \quad \text{We} = \frac{kc}{d_1}, \quad \sigma = \frac{d_1}{\sqrt{k_0}}, \quad M = \sqrt{\frac{\sigma_e}{\mu_e} B_0 d_1}, \\ F = \frac{q}{c d_1}, \quad \psi = \frac{\bar{\psi}}{c d_1}, \quad u = \frac{\partial \psi}{\partial y}, \quad v = -\frac{\partial \psi}{\partial x} \end{aligned} \dots (2.19)$$

The conditions in (2.1) can be written as

$$h_1 = 1 + a \cos(2\pi x), \quad h_2 = -d - b \cos(2\pi x + \phi), \quad \dots (2.20)$$

Using the above non-dimensional quantities and the long wavelength approximation the basic equations reduce to

$$\frac{dp}{dx} = \frac{\partial S_{xx}}{\partial y} - \sigma^2 \left(\frac{\partial \psi}{\partial y} + 1 \right), \quad \dots (2.21)$$

$$\frac{\partial p}{\partial y} = 0, \quad \dots (2.22)$$

$$f S_{xx} = 2 we S_{xy} \frac{\partial^2 \psi}{\partial y^2}, \quad f S_{xx} = 2 we S_{xy} \frac{\partial^2 \psi}{\partial y^2}, \quad f S_{yy} = 0, \quad f S_{zz} = 0 \quad \dots (2.23)$$

$$f S_{xx} = -we \frac{\partial^2 \psi}{\partial y^2} S_{yy} + \frac{\partial^2 \psi}{\partial y^2}, \quad \dots (2.24)$$

and the non-dimensional boundary conditions are

$$\psi = \frac{F}{2}, \quad \frac{\partial \psi}{\partial y} = -1 \text{ at } y = h_1 = 1 + a \cos(2\pi x), \quad \dots (2.25)$$

$$\psi = -\frac{F}{2}, \quad \frac{\partial \psi}{\partial y} = -1 \text{ at } y = h_2 = -d - b \cos(2\pi x + \phi), \quad \dots (2.26)$$

where F is the mean flow rate in the wave frame. The flux at any axial station in the fixed frame is

$$Q = \int_{h_2}^{h_1} (u+1) dy = h_1 - h_2 + F. \quad \dots (2.27)$$

The average volume flow rate over one period of the peristaltic wave is defined as

$$\Theta = \frac{1}{T} \int_0^T Q dt = \frac{1}{T} \int_0^T (h_1 - h_2 + F) dt = F + 1 + d. \quad \dots (2.28)$$

From the equation (2.23) we have $S_{yy} = 0$, $S_{zz} = 0$ and from equation (2.21) we get

$$S_{xy} = y \frac{dp}{dx} + \sigma^2 (\psi + y + 1) \quad \dots (2.29)$$

With the help of (2.23) and (2.24) we can write

$$f S_{xx} = 2 we S_{xy}^2 \quad \dots (2.30)$$

From the equations (2.17), (2.23) and (2.29) we obtain

$$\frac{\partial^2 \psi}{\partial y^2} = S_{xy} 2 \varepsilon W e^2 S_{xy}^3, \quad \dots (2.31)$$

Substituting (2.29) into (2.31) we get

$$\frac{\partial^2 \psi}{\partial y^2} = y \frac{dp}{dx} + (\sigma^2 + M^2)(\psi + y + 1) + 2 \varepsilon W e^2 \left(y \frac{dp}{dx} + (\sigma^2 + M^2)(\psi + y + 1) \right)^3 \quad \dots (2.32)$$

PERTURBATION SOLUTION

Equation (2.32) is non-linear, its exact solution is not possible, and hence we employ the perturbation technique to find the solution. For perturbation solution, we expand the flow quantities in a power series of the small parameter We^2 as follows:

$$\left. \begin{aligned} F &= F_0 + We^2 F_1 + O(We^4), \\ \frac{dp}{dx} &= \frac{dp_0}{dx} + We^2 \frac{dp_1}{dx} + O(We^4), \\ \psi &= \psi_0 + We^2 \psi_1 + O(We^4), \\ \phi &= \phi_0 + We^2 \phi_1 + O(We^4) \end{aligned} \right\} \quad \dots (3.1)$$

Using the above expressions in equations (2.25), (2.26) and (2.32), we obtain a system of equations of different orders.

3.1. System of order We^0

The governing equations and boundary conditions of the zeroth-order problem are

$$\frac{\partial^2 \psi_0}{\partial y^2} = y \frac{dp_0}{dx} + (\sigma^2 + M^2)(\psi_0 + y + 1) \quad \dots (3.2)$$

$$\psi_0 = \frac{F_0}{2}, \quad \frac{\partial \psi_0}{\partial y} = -1 \text{ at } y = h_1 = 1 + a \cos(2\pi x), \quad \dots (3.3)$$

$$\psi_0 = -\frac{F_0}{2}, \quad \frac{\partial \psi_0}{\partial y} = -1 \text{ at } y = h_2 = -d - b \cos(2\pi x + \phi), \quad \dots (3.4)$$

The solution of the zeroth-order problem is given by

$$\psi_0 = C_1 e^{Ay} + C_2 e^{-Ay} - \left(\frac{1}{A^2} \frac{dp_0}{dx} + 1 \right) y^{-1} \quad \dots (3.5)$$

and the axial velocity is

$$u_0 = AC_1 e^{Ay} - AC_2 e^{-Ay} - \left(\frac{1}{A^2} \frac{dp_0}{dx} + 1 \right) \quad \dots (3.6)$$

3.2. System of order We^2

The governing equations and boundary conditions of the first-order problem are

$$\frac{\partial^2 \psi_1}{\partial y^2} = y \frac{dp_1}{dx} + (\sigma^2 + M^2)(\psi_1 + y + 1) + 2\epsilon We^2 \left(y \frac{dp_1}{dx} + (\sigma^2 + M^2)(\psi_1 + y + 1) \right)^3 \quad \dots (3.7)$$

$$\psi_1 = \frac{F_1}{2}, \quad \frac{\partial \psi_1}{\partial y} = -1 \quad \text{at } y = h_1 = 1 + a \cos(2\pi x), \quad \dots (3.8)$$

$$\psi_1 = -\frac{F_1}{2}, \quad \frac{\partial \psi_1}{\partial y} = -1 \quad \text{at } y = h_2 = -d - b \cos(2\pi x + \phi), \quad \dots (3.9)$$

The solution of the first-order problem is given by

$$\begin{aligned} \psi_1 = & C_3 e^{Ay} + C_4 e^{-Ay} - \frac{P_1 y}{A^2} - L_2^3 (y^3 + 6/A^2) / A^2 + 3L_2^2 (y^2 + 2/A^2) - L_2 L_7 A^2 y \\ & + L_3 P_0 e^{2Ay} (y - (4/3A)) / 3A^2 - L_3 L_4 e^{2Ay} / A^2 + L_5 P_0 e^{-2Ay} (y + (4/3A)) / 3A^2 - L_4 L_5 e^{-2Ay} / A^2 \\ & + 3A^2 C_1 e^{Ay} ((L_2^2 / 2A)(y^3 / 3) - (y^2 / 2A) + (y / 2A^2)) - AL_2 ((y^2 / 2) - (y / 2A)) + A^3 y / 2 \\ & + 3A^2 C_2 e^{-Ay} ((L_2^2 / 2A)(y^3 / 3) + (y^2 / 2A) + (y / 2A^2)) + AL_2 ((y^2 / 2) + (y / 2A)) - A^3 y / 2 \\ & + (A^4 / 8)(C_1^3 e^{3Ay} - C_2^3 e^{-3Ay}) - (L_6 / A^2) \quad \dots (3.10) \end{aligned}$$

and the corresponding first-order axial is velocity given by

$$\begin{aligned} u_1 = & C_3 A e^{Ay} - C_4 A e^{-Ay} - \frac{P_1}{A^2} - L_2^3 (3y^2 + 6/A^2) / A^2 + 6L_2^2 y - L_2 L_7 A^2 \\ & + 2L_3 P_0 e^{2Ay} (y - (4/3A)) / 3A + (L_3 P_0 e^{2Ay} / 3A^2) - (2L_3 L_4 e^{2Ay} / 3A) \\ & + (L_5 P_0 e^{-2Ay} / 3A^2) (-2A(y + (4/3A)) + 1) + (2L_4 L_5 e^{-2Ay} / 3A) \\ & + 3A^2 C_1 e^{Ay} ((L_2^2 / 2A)(y^2 - (y/A) + (1/2A^2)) - AL_2 (y - (1/2A)) + A^3 / 2) \\ & + 3A^3 C_1 e^{Ay} ((L_2^2 / 2A)(y^3 / 3 - (y^2 / 2A) + (y / 2A^2)) - AL_2 ((y^2 / 2) - (y / 2A)) + A^3 y / 2) \\ & + 3A^2 C_2 e^{-Ay} ((-L_2^2 / 2A)(y^2 + (y/A) + (1/2A^2)) + AL_2 (y + (1/2A)) + A^3 / 2) \\ & + 3A^3 C_2 e^{-Ay} ((-L_2^2 / 2A)(y^3 / 3 + (y^2 / 2A) + (y / 2A^2)) + AL_2 ((y^2 / 2) + (y / 2A)) - A^3 y / 2) \\ & + 3A^5 / 8 (C_1^3 e^{3Ay} - C_2^3 e^{-3Ay}) \quad \dots (3.11) \end{aligned}$$

The final expression for the axial velocity is given by

$$u = u_0 + We^2 u_1. \quad \dots (3.12)$$

The pressure gradient is obtained as

$$\frac{dp}{dx} = \frac{dp_0}{dx} + We^2 \frac{dp_1}{dx} \quad \dots (3.13)$$

where $\frac{dp_0}{dx} = \frac{A^3 (F_0 - (h_1 - h_2) \sinh A(h_1 - h_2))}{(1 - \cosh A(h_1 - h_2) - A(h_1 - h_2) \sinh A(h_1 - h_2))}$, $\dots (3.14)$

$$\frac{dp_1}{dx} = \frac{A^3 (F_1 A \sinh A(h_1 - h_2) - L_{106})}{1 - A \cosh A(h_1 - h_2) - (h_1 - h_2) A \sinh A(h_1 - h_2)}$$
, $\dots (3.15)$

The non-dimensional pressure rise and the non-dimensional friction forces per unit wave length in the wave frame are given by

$$\Delta p = \int_0^1 \frac{dp}{dx} dx \quad \dots (3.16)$$

$$F_1 = \int_0^1 (-h_1) \frac{dp}{dx} dx \quad \dots (3.17)$$

$$F_2 = \int_0^1 (-h_2) \frac{dp}{dx} dx \quad \dots (3.18)$$

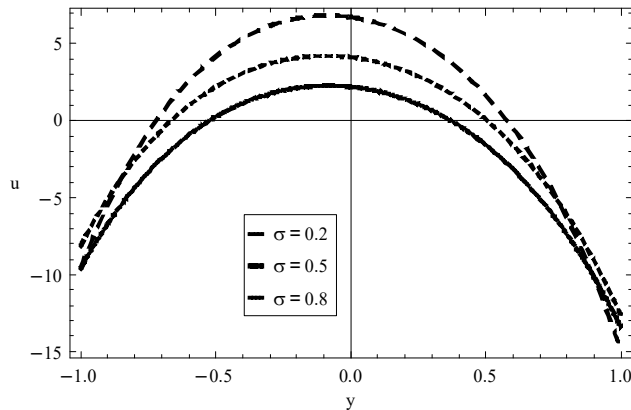


Fig. 1. Velocity profiles for different permeability ‘ σ ’ and fixed $x = 0.1, a = 0.3, d = 1, \phi = \pi/8, We = 0.5, b = 0.3, F = 1.5, M = 1.7, \epsilon = 0.05$

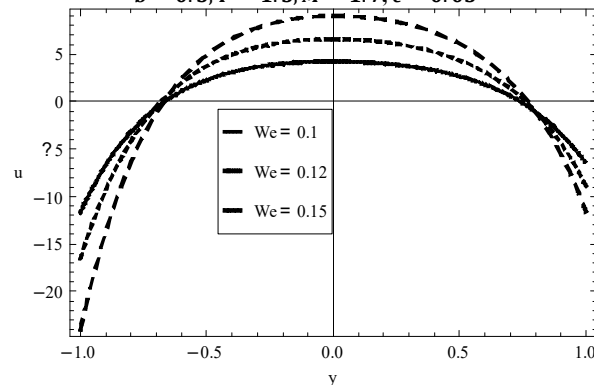


Fig. 2. Velocity profiles for different Weissenberg number ‘ We ’ and fixed $x = 0.2, a = 0.2, d = 1, \phi = \pi/6, b = 0.35, \sigma = 1.5, F = 1.5, M = 3, \epsilon = 0.05$.

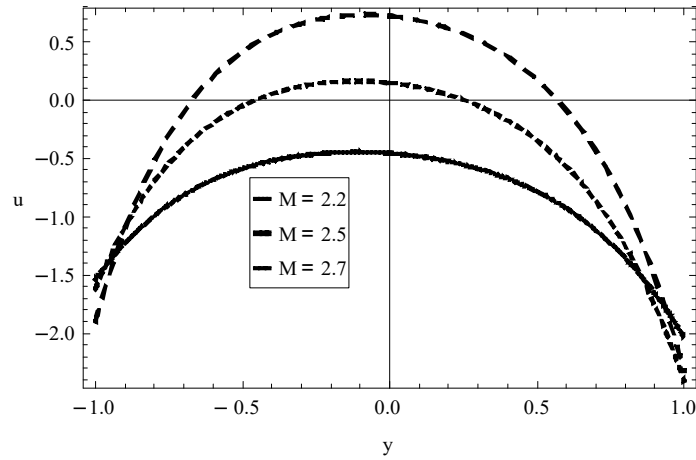


Fig. 3. Velocity profiles for different Hermattan number ' M ' and fixed $x = 0.1$, $a = 0.25$, $d = 1$, $\phi = \pi/8$, $b = 0.3$, $\sigma = 1.2$, $F = 1.5$, $We = 0.07$, $\epsilon = 0.05$.

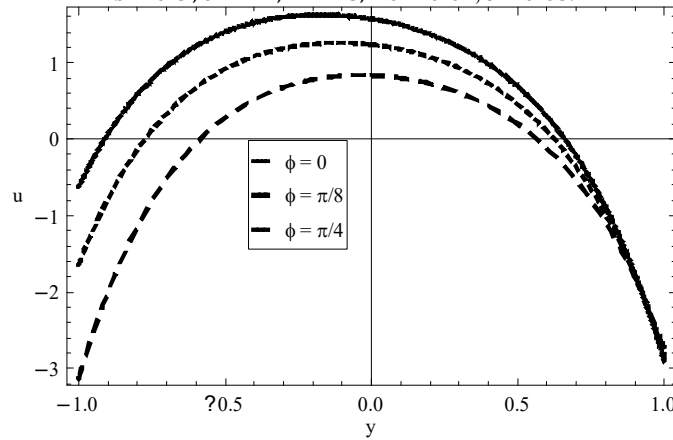


Fig. 4. Velocity profiles for different phase difference ' ϕ ' and fixed $x = 0.1$, $M = 3$, $d = 1$, $b = 0.4$, $a = 0.25$, $\sigma = 1.2$, $F = 1.5$, $We = 0.09$, $\epsilon = 0.05$.

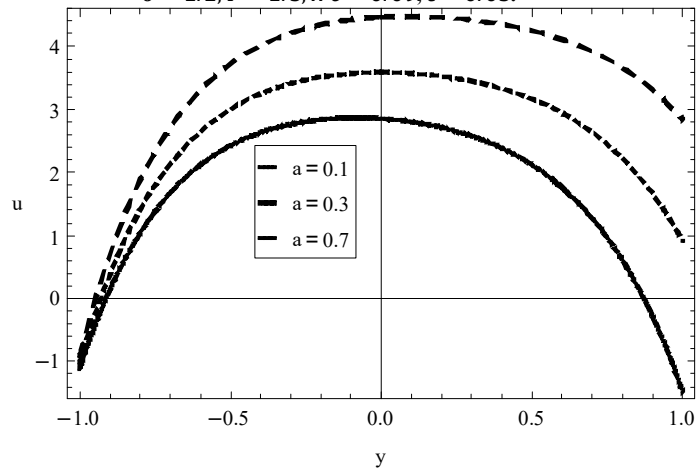


Fig. 5. Velocity profiles for different amplitude ' a ' and fixed $x = 0.01$, $d = 1$, $b = 0.3$, $\sigma = 1.1$, $F = 0.5$, $We = 0.07$, $\epsilon = 0.05$, $\phi = \pi/8$.

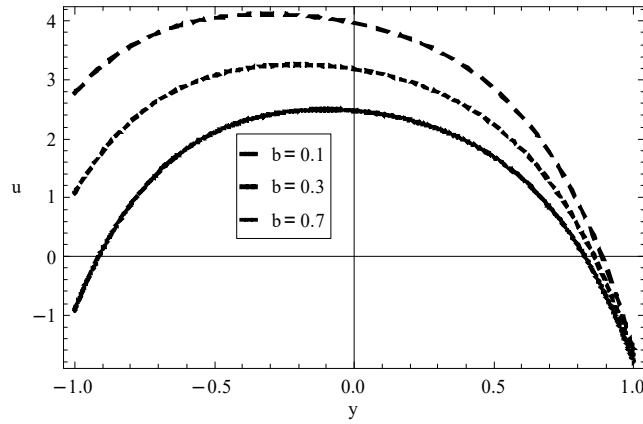


Fig. 6. Velocity profiles for different amplitude 'b' and fixed $x = 0.01, d = 1, a = 0.3, \sigma = 1.5, F = 1.5, We = 0.09, \epsilon = 0.05, \phi = \pi/8$.

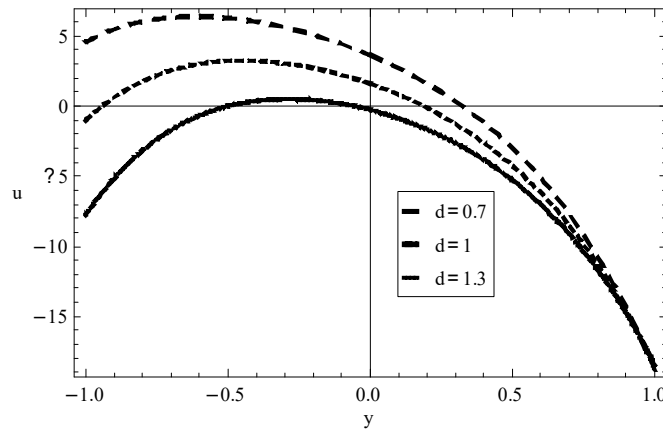


Fig. 7. Velocity profiles for different 'd' and fixed $x = 0.05, a = 0.4, b = 0.4, \sigma = 1.5, M = 1.5, F = 1.5, We = 0.25, \epsilon = 0.05, \phi = \pi/6$.

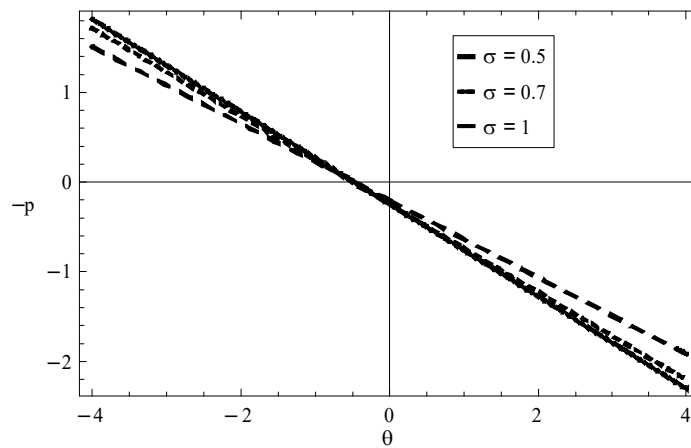


Fig. 8. Variation of pressure rise for different 'sigma' and fixed $a = 0.2, b = 0.3, We = 0.02, \epsilon = 0.1, d = 1.1, \phi = \pi/6$.

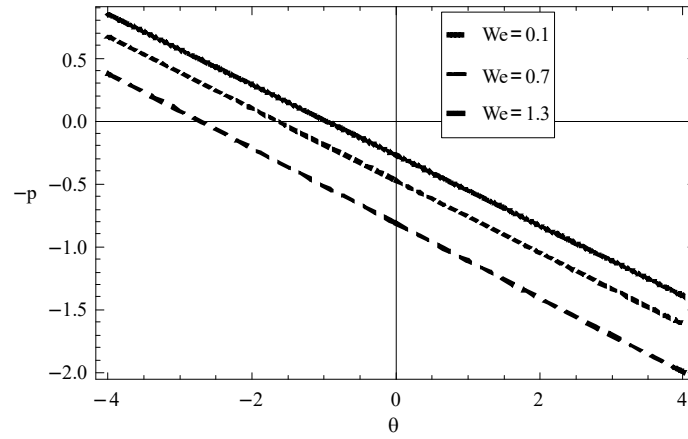


Fig. 9. Variation of pressure rise for different 'We' and fixed $a = 0.3, b = 0.5, \epsilon = 0.3, d = 1.2, \sigma = 1.5, \phi = \pi/6, M = 0.9$.

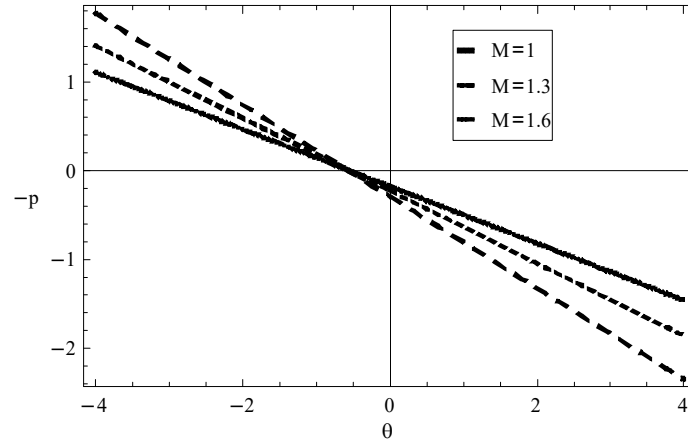


Fig. 10. Variation of pressure rise for different 'M' and fixed $a = 0.3, b = 0.3, \epsilon = 0.3, d = 1, \phi = \pi/6, We = 0.01$.

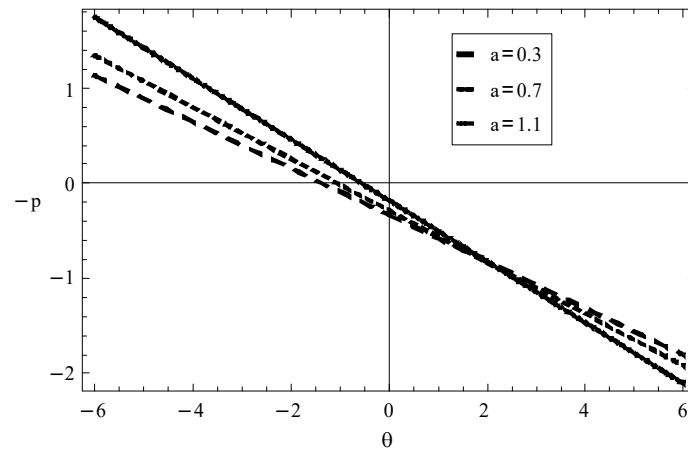


Fig. 11. Variation of pressure rise for different 'a' and fixed $We = 0.01, b = 0.4, \epsilon = 0.3, d = 1, \phi = \pi/8, M = 1$.

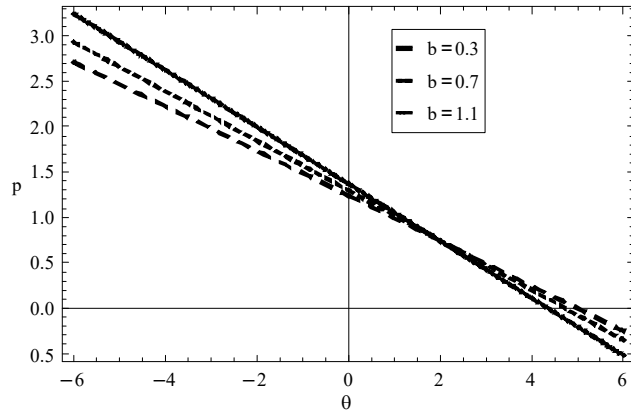


Fig. 12. Variation of pressure rise for different 'b' and fixed $We = 0.1, a = 0.3, \epsilon = 0.3, d = 0.9, \phi = \pi/6, M = 1$.

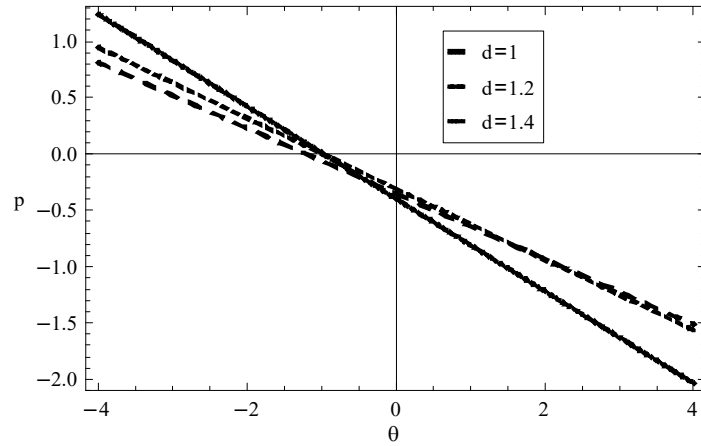


Fig. 13. Variation of pressure rise for different 'd' and fixed $We = 0.01, a = 0.3, \epsilon = 0.3, b = 0.3, \phi = \pi/6, M = 1$.

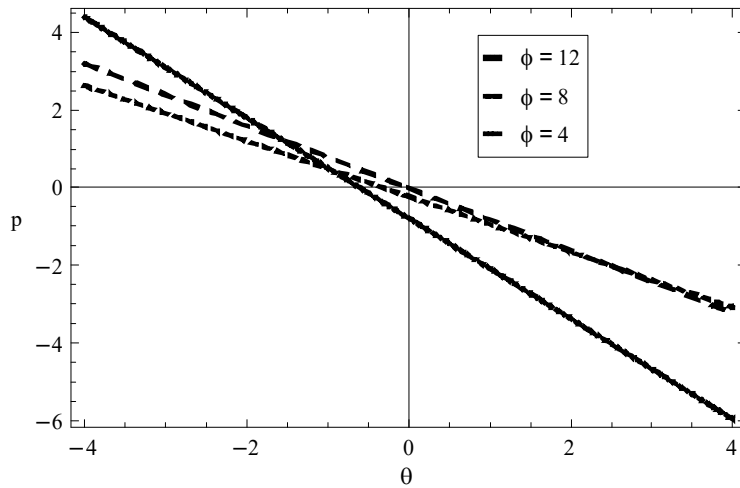


Fig. 14. Variation of pressure rise for different ' ϕ ' and fixed $We = 0.01, a = 0.3, M = 2, \epsilon = 0.3, b = 0.2, d = 1$.

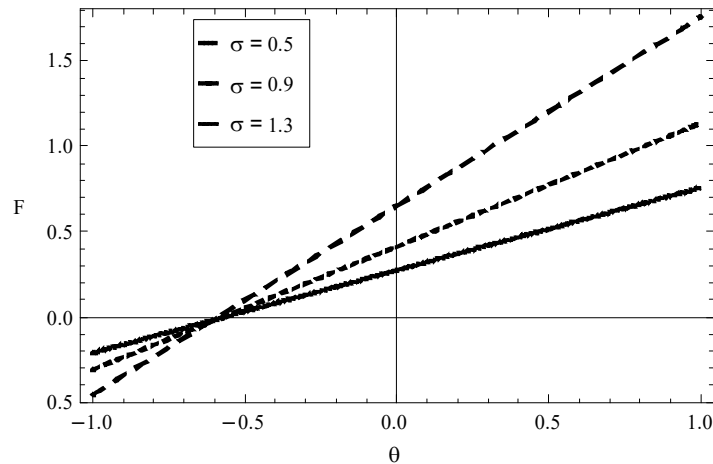


Fig. 15. Variation of frictional force (at $y = h_1$) for different σ and fixed $We = 0.02, a = 0.3, M = 1, \epsilon = 0.1, b = 0.3, d = 1, \phi = \pi/8$.

RESULTS AND DISCUSSIONS

The effects of various physical parameters like permeability σ , magnetic field, phase difference ϕ and amplitudes a and b on velocity and pressure rise are calculated using equation (3.11) and (3.13) and are shown through graphs. Fig. 1 shows that velocity increases with increasing permeability parameter σ . Also it is observed that velocity profiles are parabolic for fixed $x = 0.1, a = 0.3, d = 1, \phi = \pi/8, We = 0.5, b = 0.3, F = 1.5, M = 1.7, \epsilon = 0.05$. From Fig. 2, the velocity profile for different values of Weissenberg number We for fixed $x = 0.2, a = 0.2, M = 3, \epsilon = 0.05, b = 0.35, d = 1, \phi = \pi/6, \sigma = 1.5$, is parabolic and velocity decreases as We increases for fixed y . From Fig. 3, the velocity profile for different values of M for fixed $x = 0.1, a = 0.25, \epsilon = 0.05, b = 0.3, d = 1, We = 0.07, F = 1.5, \phi = \pi/6, \sigma = 1.2$, is parabolic and velocity decreases as We increases for fixed y . From Fig. 4, it is observed that the velocity profile for different values ' ϕ ' and for fixed $x = 0.1, d = 1, b = 0.4, a = 0.25, \sigma = 1.2, F = 1.5, We = 0.09, M = 3, \epsilon = 0.05$ is parabolic and velocity decreases as ϕ increases for fixed y . Fig. 5 and Fig. 6 depict that for fixed $x = 0.01, d = 1, M = 1, \sigma = 1.1, F = 0.5, We = 0.07, \epsilon = 0.05, \phi = \pi/8$ and varying amplitudes a and b the velocity is increasing for fixed y and it is parabolic.

We have calculated the pressure rise Δp in terms of the mean flow rate θ from equation (3.16). Fig. 8 shows the effect of σ and Fig. 9 M on Δp . We observe that for a given θ , the pressure rise decreases with increasing σ initially and coincide at a particular point and after this point the situation is reversed. The effect of M is shown in Fig. 10. It can be seen that the pressure rise increases with an increase in M . From Fig. 13 we observe that the pressure rise decreases with increasing ϕ . From Fig. 14, we notice that the frictional forces have the opposite behaviour when compared with the pressure rise.

REFERENCES

1. Latham, T.W., "Fluid Motion in a Peristaltic Pumps", *M.S. Thesis*, MIT, Cambridge, MA (1966).
2. Barton, C., Raynor, S., "Peristaltic flow in tubes", *Bull. Math. Biophys.*, **30**, 663–680 (1968).
3. Yin, F.C.P., Fung, Y.C., "Peristaltic waves in circular cylindrical tube's", *J. Appl. Mech.*, **36**, 579–587 (1969).

4. Colgan, T., Terrill, R.M., "On peristaltic transport of fluids", *J. Theoret. Appl. Mech.*
5. Yin, F.C.P., Fung, Y.C., "Comparison of theory and experiment in peristaltic transport", *J. Fluid Mech.*, **47**, 93–112 (1971).
6. Misra, J.C., Pandey, S.K., "Peristaltic transport of blood in small vessels: Study of mathematical model", *Comput. Math. Applic.*, **43**, 1183–1193 (2002).
7. Mishra, M., Rao, A.R., "Peristaltic transport of a Newtonian fluid in an asymmetric channel", *J. Appl. Math. Phys. (ZAMP)*, **54**, 532–550 (2003).
8. Reddy, M.V.S., Rao, A.R., Sreenadh, S., "Peristaltic transport of a power-law fluid in an asymmetric channel", *Int. J. Non-lin. Mech.*, **42**, 1153–1161 (2007).
9. Ali, N., Hayat, T., "Peristaltic flow of a micropolar fluid in an asymmetric channel", *Comput. Math. Appl.*, **55**, 589–608 (2008).
10. Rani, P.N., Sarojamma, G., "Peristaltic transport of a Casson fluid in an asymmetric channel", *Australas. Phys. Eng. Sci. Med.*, **27 (2)**, 49–59 (2004).
11. Eytan, O., Elad, D., "Analysis of intra-Uterine fluid motion induced by uterine contraction's", *Bull. Math. Biol.*, **61**, 221–238 (1999).
12. Shukla, B., Gupta, S.P., "Peristaltic transport of a powerlaw fluid with variable consistency", *J. Biomech. Eng.*, **104**, 182–186 (1982).
13. Hayat, T., Wang, Y., Siddiqui, A.M., Hutter, K., Asghar, S., "Peristaltic transport of a third-order fluid in a circular cylindrical tube", *Math. Models Meth. Appl. Sci.*, **12 (12)**, 1691–1706 (2002).
14. Haroun, M.H., "Non linear peristaltic flow of a fourth grade fluid in an inclined asymmetric channel", *Comput. Maier. Sci.*, **39**, 324–333 (2007).
15. Hayat, T., Wang, Y., Siddiqui, A.M., Hutter, K., "Peristaltic motion of a Johnson–Segalman fluid in a planar channe", *Math. Prob. Eng.*, 1–23 (2003).
16. Misra, J.C., Maiti, S., Shit, G.C., "Peristaltic transport of a physiological fluid in an asymmetric porous channel in the presence of an external magnetic field", *J. Mech. Med. Biol.*, **8 (4)**, 507–525 (2008).
17. Shit, G.C., Roy, M., Ng, E.Y.K., "Effect of induced magnetic field on peristaltic flow of a micropolar fluid in an asymmetric channel", *Int. J. Numer. Meth. Biomed. Eng.*, **26 (11)**, 1380–140 (2010).
18. Raju, K. K. and Devanatham, R., "Peristaltic motion of a non-Newtonian fluid", *Rheologica Acta*, **13**, 944-948 (1974).
19. Ravi Kumar, Y. V. K., Krishna Kumari, S. V. H. N., Raman Murthy, M. V., Sreenadh, S., "Unsteady peristaltic pumping in a finite length tube with permeable wall", *Trans. ASME, Journal Fluids Engineering*, **32**, 1012011-1012014 (2010).
20. Ravi Kumar, Y. V. K., Krishna Kumari, P. S. V. H. N., Ramana Murthy, M. V., Chenna Krishna Reddy M., "Peristaltic pumping of a magnetohydrodynamic Casson fluid in an inclined channel", *Advances in Applied Science Research*, **2(2)**, 428-436 (2011).
21. Ravi Kumar, Y. V. K., Krishna Kumari, P. S. V. H. N., Ramana Murthy, M. V., S., Sreenadh., "Peristaltic pumping of a Jeffrey fluid under the effect of a magnetic field in an inclined channel", *Applied Mathematical Sciences*, **5**, 9, 447-458 (2011).
22. Ravi Kumar, Y. V. K., Krishna Kumari, P. S. V. H. N., Ramana Murthy, M. V., S., Sreenadh., "Effects of Slip and Heat Transfer on the Peristaltic Pumping of a Williamson Fluid in an Inclined Channel", *Int. J. Appl. Sci. Eng.*, **12**, 2, 155 (2014).

